DOI: 10.1515/FAS-2017-0011
FATIGUE OF AIRCRAFT STRUCTURES (2017)
S. 137–155

DESIGN AND STRENGTH ANALYSIS OF CURVED-ROOT CONCEPT FOR COMPRESSOR ROTOR BLADE IN GAS TURBINE

Wojciech Wdowiński[1], Elżbieta Szymczyk[2], Jerzy Jachimowicz[3], Grzegorz Moneta[4]

[1]Ansaldo Energia, Switzerland,
[2]Military University of Technology, Warsaw
[3]Military University of Technology, Warsaw
[4]Ansaldo Energia, Switzerland

Abstract

The motivation of the article is fatigue and fretting issue of the compressor rotor blades and disks. These phenomena can be caused by high contact pressures leading to fretting occurring on contact faces in the lock (blade-disk connection, attachment of the blade to the disk). Additionally, geometrical notches and high cyclic loading can initiate cracks and lead to engine failures. The paper presents finite element static and modal analyses of the axial compressor 3rd rotor stage (disk and blades) of the K-15 turbine engine. The analyses were performed for the original trapezoidal/dovetail lock geometry and its two modifications (new lock concepts) to optimize the stress state of the disk-blade assembly. The cyclic symmetry formulation was used to reduce modelling and computational effort.

Keywords: finite element method, turbine engine, rotor disk, rotor blades, blade-disc connection, shape optimization.

1. INTRODUCTION

A compressor is one of the most important components of a turbine engine. Its main function is introducing the optimum amount of compressed air to the combustion chamber, where it is combined with fuel mist, then the mixture burns, drives the turbine and generates the thrust. The compressor section in the aircraft turbine engine is built from a series of stages (rotating and stationary). Each rotor stage consists of a rotor disk and the blades [1].

The blades are attached to the disk rim with the lock (where the blade root is fitted into the groove/slot in the disk). The most frequent reasons of compressor failures are fatigue and fretting phenomena occurring in the lock zone. Both of these phenomena are mainly caused by the occurrence of high magnitudes of

cyclic stresses, contact pressures and vibrations leading to a cyclic slip and wear in the contact area. In addition, complex shapes of these parts result in localstress concentrations as well as the formation of micro-cracks which can propagate during the operation time/service life of the engine [1]. An exemplary pre-cracked lock is shown in Fig. 1.

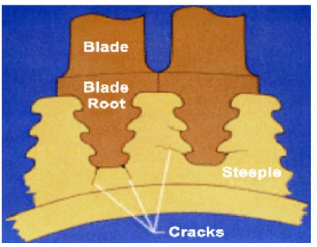

Fig. 1. Cracks in the fir-tree lock/attachment method[2]

These conditions together with high inertial loads applied to the assembly can result in a fatigue failure caused by uncontrolled fatigue cracks initiating at a stress concentration location [3, 13] (Fig. 2).

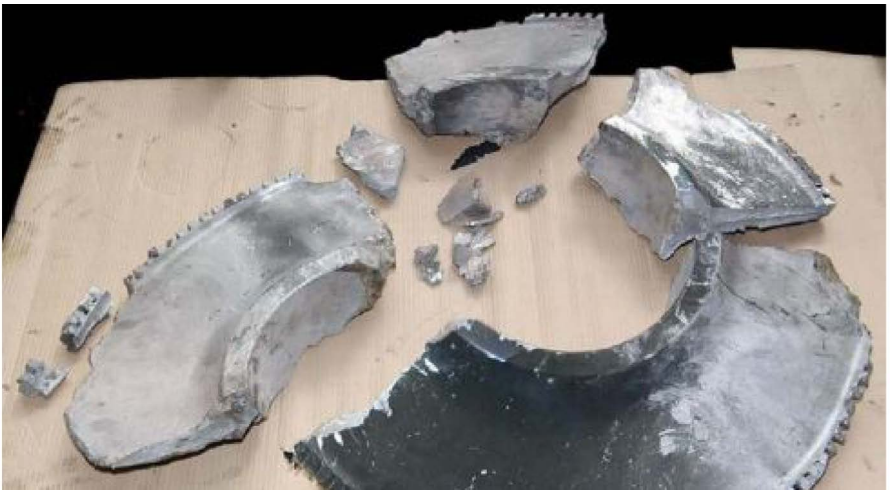

Fig. 2. Disk failure in the aircraft engine [3]

In order to solve the durability problem of aircraft engine components, a stress to material strength ratio in the whole volume of the parts needs to be reduced. In practice, the improvement methods may be as follows [4]:

- use of high strength materials,
- reduction of stress magnitude, especially in the disk:
  - use of dampers to reduce vibrations, decrease the slip and stress amplitudes,

– geometry modification (shape optimization) of the lock (blade to disk attachment method).

In the paper, the design of a blade attachment to the rim of the turbine jet engine rotor disk has been proposed and analysed.

2. CAD AND FEM MODELS OF THE COMPRESSOR 3RD ROTOR STAGE

2.1 Original lock geometry (model Ver.0)

The main modelling problem of the compressor's parts is their complex shape. Development of CAD and FEM models needs to be performed carefully to capture all important features and, simultaneously, apply possible simplifications to reduce the FE mesh size. An engineer's experience and skills are important during this step.

A geometrical model of the K-15 compressor 3rd rotor stage was developed based on the technical documentation of the engine in CATIA V5, Dassault System software. The compressor rotor parts (blade and disk) are shown in Fig. 3 and 4, respectively. Figure 5 shows approximate dimensions of each component in [mm].

Modelling of both the blade and the disk in CATIA required performing a number of necessary steps to reproduce the CAD geometry from the technical paper documentation. Additionally, in order to reduce the size of the model and, consequently, computational time, the cyclic symmetry formulation was used. A specific cut of the geometry allowed creating a repeatable sector of a disk with one blade (Fig. 6).

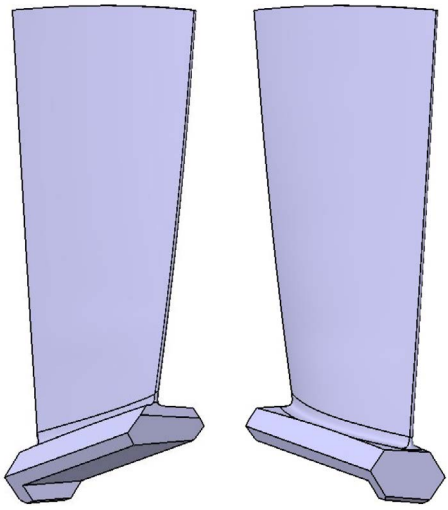

Fig. 3. Compressor 3rd stage rotor blade with a trapezoidal/dovetail root

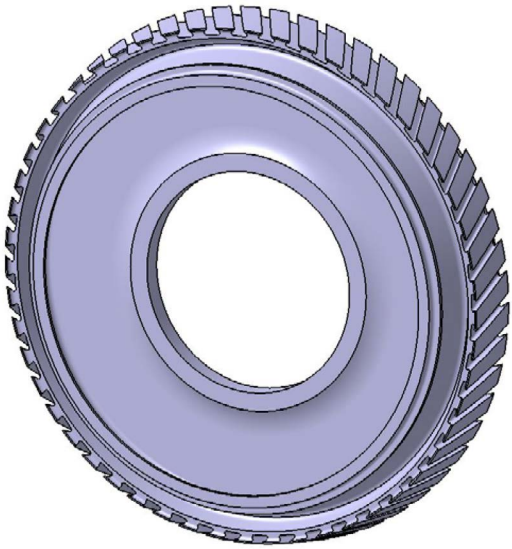

Fig. 4. Compressor 3rd stage rotor disk

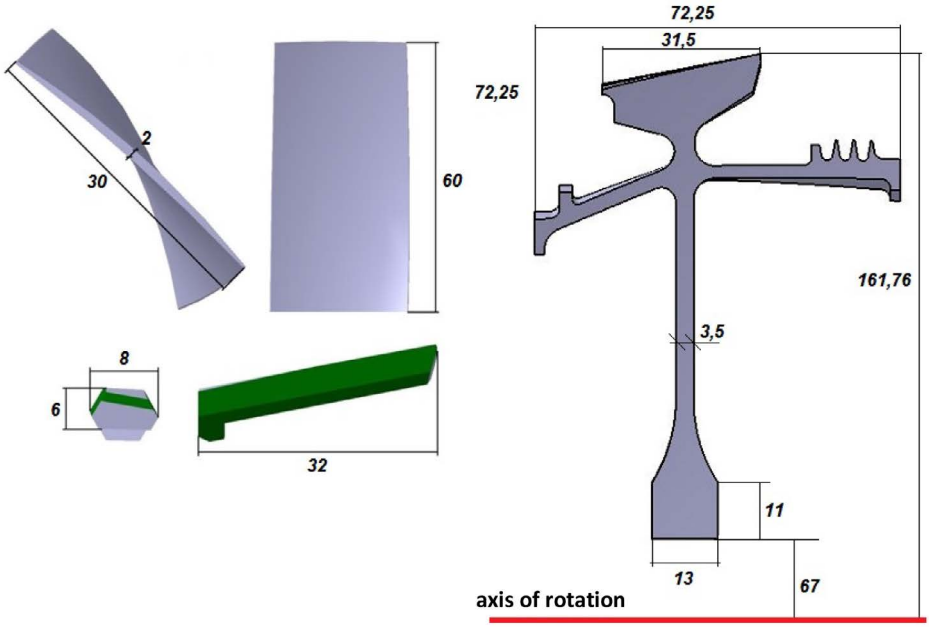

Fig. 5. Approximate dimensions of the rotor components

Fig. 6. Cyclic symmetry model of the compressor 3rd rotor stage

2.2 Conceptual models of the lock (blade attachment to the disk)

There are both advantages and disadvantages to the original geometry of the lock used in the compressor 3rd rotor stage. One of the advantages to this solution (trapezoidal/dovetail lock geometry) is its standard shape allowing for application of a relatively simple manufacturing process. A curved blade aerofoil tends to unbend and untwist under centrifugal load, while the straight trapezoidal root limits the deformation. The above described behaviour is one of the reasons for designing a more sophisticated blade-disk attachment method and create more competitive products.

Curved lock geometry may overcome, to some extent, the disadvantages of the original solution. The main purpose of applying this geometry is to obtain more uniform contact pressure distribution, reduce the stress concentration in both the elements and improve both the fatigue performance (cyclic durability) of the assembly and the engine lifetime. However, it should be noted that more sophisticated geometrical shapes require a more advanced and expensive manufacturing technology.

Curved geometry of the blade root and the disk groove/slot was created by extruding the baseline root cross-section along the characteristic curve parallel to the camber line of the aerofoil of the bottom blade section (Fig. 7).

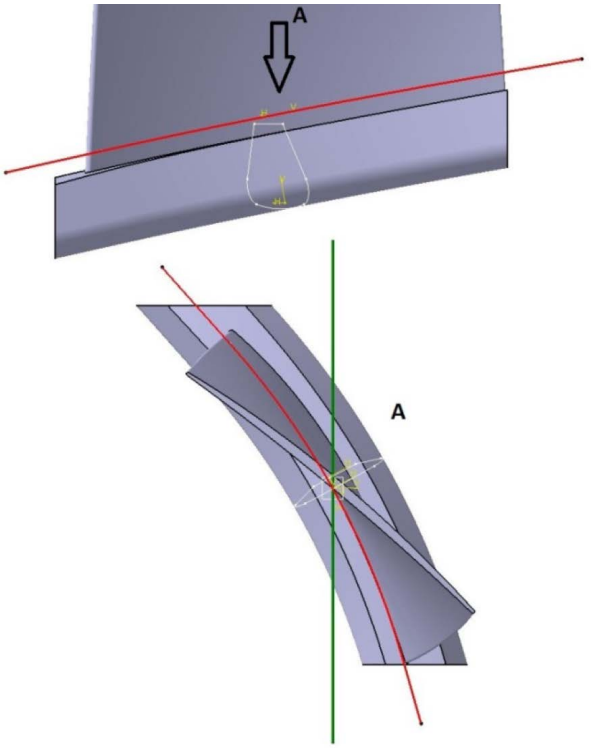

Fig. 7. Curved root (green line – rotation axis; red line – camper line of the aerofoil of the bottom blade section)

The result of the first modification (curving the original root geometry – model Ver.1) is shown in Fig. 8. The modification of the disk groove/slot is presented in Fig. 9.

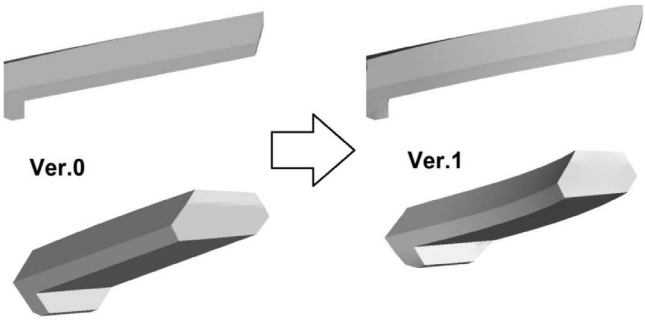

Fig. 8. Curved shape of the blade root – model Ver.1

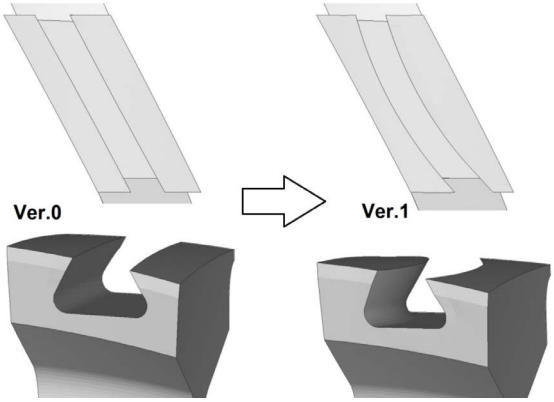

Fig. 9. Curved shape geometry of the disk groove/slot – model Ver.1

The next concept was an additional improvement to the groove bottom shape – model Ver.2 (Fig. 10). The root of the blade remained the same as in model Ver.1.

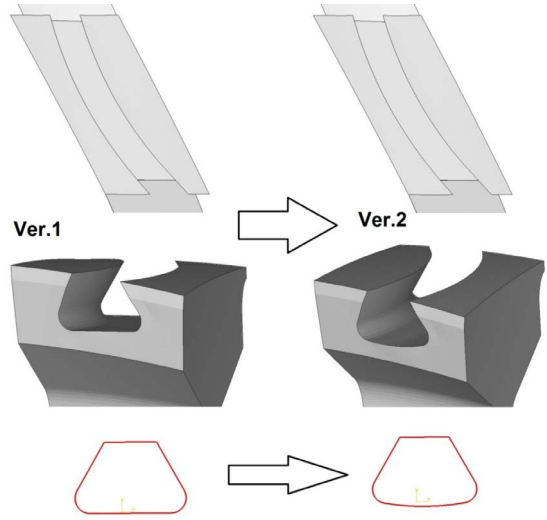

Fig. 10. Curved shape geometry of the disk groove/slot – models Ver.1 and Ver.2

3. MATERIALS USED FOR THE COMPRESSOR ROTOR

Design of modern and innovative materials is required for development of more competitive and modern engines. The compressor rotor blade is made from WT3-1 titanium alloy. It is a two-phase titanium-based martensitic alloy commonly used in aircraft constructions. The chemical composition of the WT3-1 titanium alloy is shown in Table 1 [5].

Table 1. Chemical composition of WT3-1 titanium alloy [5]

Alloy	Al [%]	Mo [%]	Cr [%]	Si [%]	Fe [%]
WT3-1	5.5 – 7.0	2.0 – 3.0	0.8 – 2.0	0.15 – 0.40	0.2 – 0.7
Alloy	Cr [%]	C [%]	Ni [%]	O [%]	N [%]
WT3-1	max. 0.5	max. 0.1	max. 0.8	max. 0.15	max. 0.05

A distinctive property of WT3-1 alloy is high corrosion resistance, especially in seawater, chloride salts, acids and organic compounds, which permits the use of this material for elements exposed to work in an aggressive environment [5].

Compressor disk material is N18K9M5TPr steel more often recognised/ found as Maraging 250. Components of this alloy shown in Tab. 2 ensure its high metallurgical purity [6].

Table 2. Chemical composition of Maraging 250 steel [6]

Alloy	Ni [%]	Co [%]	Mo [%]	Cr [%]	Cu [%]	Ti [%]
N18K9M5TPr	17.0 – 19.0	7.0 – 8.5	4.6 – 5.2	0.5	0.5	0.3 – 0.5
Alloy	Al [%]	Mn [%]	Si [%]	C [%]	S [%]	P [%]
N18K9M5TPr	0.05 – 0.15	max. 0.1	max. 0.1	max. 0.03	max. 0.01	max. 0.01

3.1 Material models used in numerical analyses

Piece-wise linear elastic-plastic material models were used for finite element calculation. Taking into account that aircraft parts should operate in elastic regime (only local plastification is allowed according to JAR-E regulations), stress magnitude below yield stress is expected. Table 3 presents material data used for numerical analyses [7, 8].

Table 3. Material data used for FE analyses of the compressor rotor [7, 8]

Material	Young Modulus [GPa]	Density [kg/m^3]	Poisson ratio [–]	$R_{0,2}$[MPa]	R_m [MPa]
WT3–1	114	4710	0,34	1128	1226
Maraging 250	186	7848	0,30	1850	1920

4. DEVELOPMENT OF FEM MODELS AND ANALYSIS OF A COMPRESSOR 3RD ROTOR STAGE – ORIGINAL LOCK GEOMETRY

At the beginning, rotor with an original lock (blade attachment to the disk) design was analysed. Discretization of geometry (finite element mesh) was performed in Altair HyperMesh [9]. The blade model was meshed with 23240 solid elements (HEX8 type, 8-node bricks, first order) and 29163 nodes. Due to a complex shape of the aerofoil, the geometrical model was firstly split into smaller sub-volumes to make discretization more precise and efficient. In addition, local mesh refinement was used at a transition zone between the blade root and the aerodynamic profile (aerofoil).

The last part subjected to discretization was the repeatable part of the compressor rotor disk. The numerical model of the part consists of 67586 solid elements HEX8 type and 79618 nodes. Similarly as in the case of the compressor blade, the geometry of the disk was divided into smaller sub-volumes to facilitate precise discretization. A cyclic symmetry formulation used in the model, requires an identical mesh on both sides of the repeatable disk part (shape of both faces and number of nodes should be the same).

Discrete models of both parts are presented in Figures 12 and 13.

The first step of the FE assessment was static analysis. The centrifugal force corresponding to 15900 rpm is the dimensional load case. The analysis was performed with the Ls-Dyna implicit solver [10] and the results are presented in a cylindrical coordinate system with a consistent unit system [N, mm, s]. The equivalent stress is presented using the Huber-Mises-Hencky formulation (H-M-H).

Stress states in the rotor blade and the disk are shown in Fig. 14 and Fig. 15–18, respectively. The displacement state of the assembly is presented in Fig. 19.

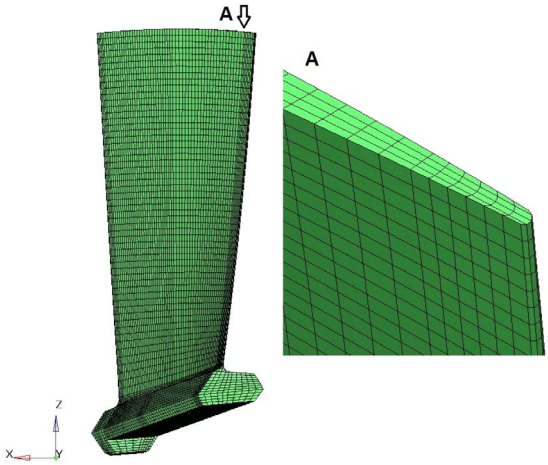

Fig. 12. FE mesh of the compressor blade with the original lock design (model Ver.0)

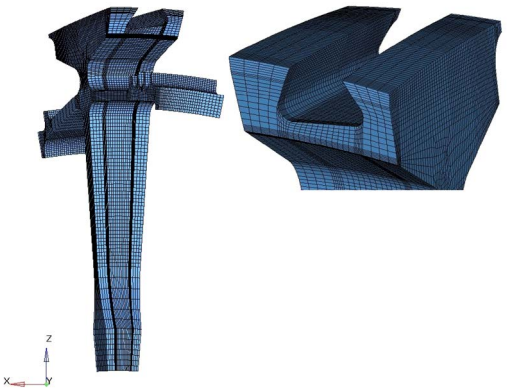

Fig. 13. FE mesh of compressor disk cyclic model with the original lock design (model Ver.0)

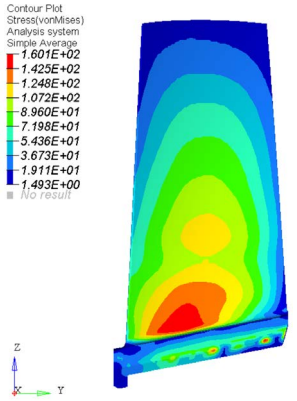

Fig. 14. Equivalent stress state (H-M-H) in the compressor blade with original lock geometry (model Ver.0). Maximum stress magnitude 160.1 MPa is obtained on the blade pressure side in the fillet zone

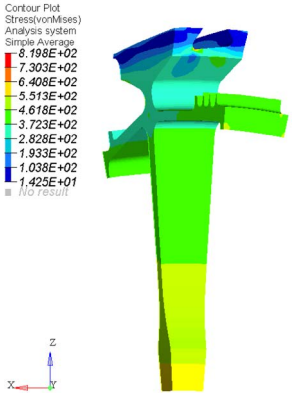

Fig. 15. Equivalent stress state (H-M-H) in the compressor disk with original lock geometry (model Ver.0). Maximum stress magnitude 819.8 MPa is obtained at the bottom of the groove/slot zone

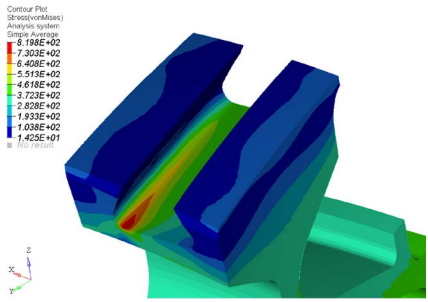

Fig. 16. Equivalent stress state (H-M-H) in the compressor disk with original lock geometry (model Ver.0). Zoom at the bottom of the groove/slot zone

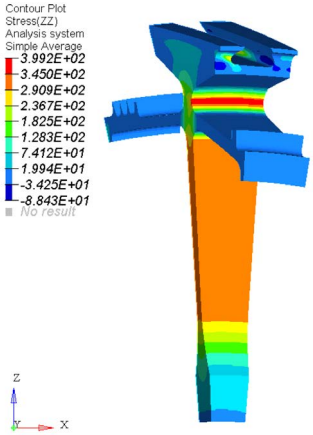

Fig. 17. Radial stress state in the compressor disk with original lock geometry (model Ver.0). Maximum stress magnitude 399.2 MPa is obtained in the neck region

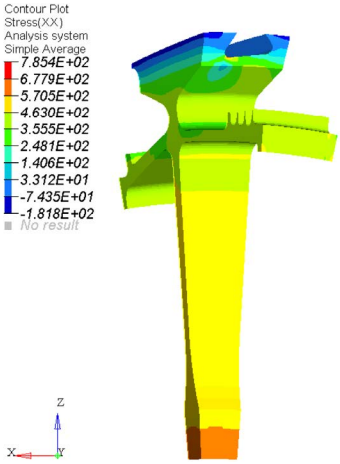

Fig. 18. Hoop stress state in the compressor disk with original lock geometry (model Ver.0). Maximum stress magnitude 785.4 MPa is obtained at the bottom of the groove/slot zone

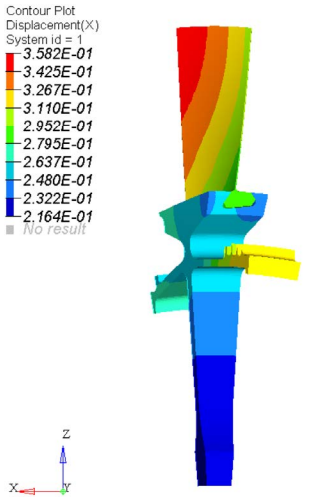

Fig. 19. Radial displacement state of the compressor rotor assembly with original lock geometry (model Ver.0). Maximum displacement magnitude is 0.36 mm

The stress state obtained from the FE analysis is consistent with analytical calculations and stress values correspond to those given in the literature [1, 11-12, 14-15]. The maximum radial displacement obtained is 0.36 mm and it is lower than the allowable displacement of 1.2 mm that ensures optimal clearance to avoid rubbing between the compressor casing and blade tips

Next, modal analysis (determination of natural frequencies and corresponding modes) of the whole rotor assembly was carried out. The initial stress conditions were taken from the static analysis and the results of the free vibration analysis are shown in Fig. 20.

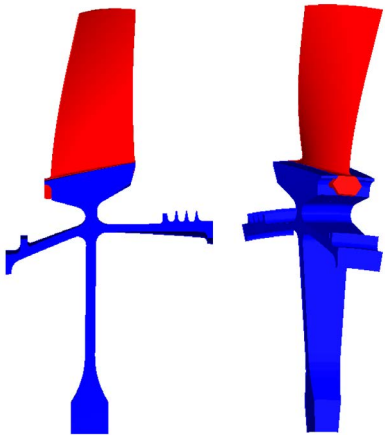

Fig. 20. 1st vibration mode of the rotor assembly with original lock geometry (model Ver.0) with frequency 843.82 Hz

5. COMPRESSOR 3RD ROTOR STAGE ASSEMBLY AFTER MODIFICATIONS

The results of the numerical analysis of the compressor 3rd rotor stage with original lock geometry show locations of the highest stress concentrations. Despite the fact that the maximum stress values are over twice as low as the corresponding yield stresses of the used materials, it is desired to reduce them in order to improve fatigue strength and safety factors. Therefore, shape modifications of the blade to disk connection (blade root and disk rim groove/ slot) have been proposed (see p. 2.2).

Considering that the meshing process of the new geometrical model of the rotor assembly requires a relatively huge effort, another technique was used to create FE models of modified designs. HyperMorph module and the morphing procedure were used to project an original FE mesh (with all boundary conditions, loads, contact definitions, etc.) to new geometries. As a result of modifications, new FE meshes were obtained for both parts (disk and blade) and both models (Ver.1 and Ver.2) (Fig. 21- 23).

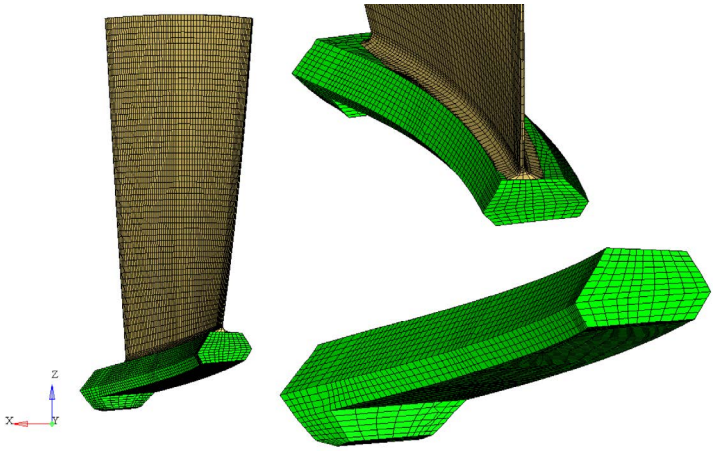

Fig. 21. FE mesh pattern of the modified rotor blade root (models Ver.1 and Ver.2)

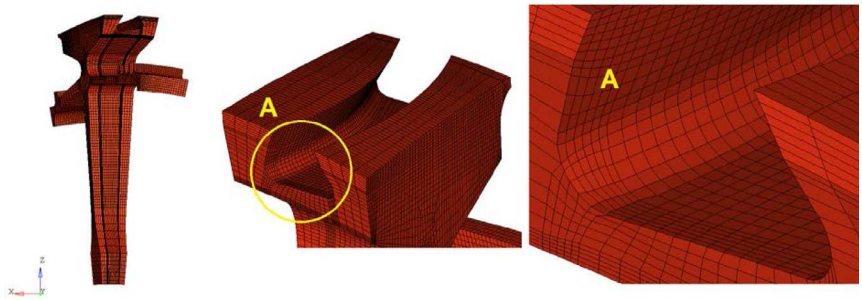

Fig. 22. FE mesh pattern of the modified rotor disc (cyclic symmetry model Ver.1)

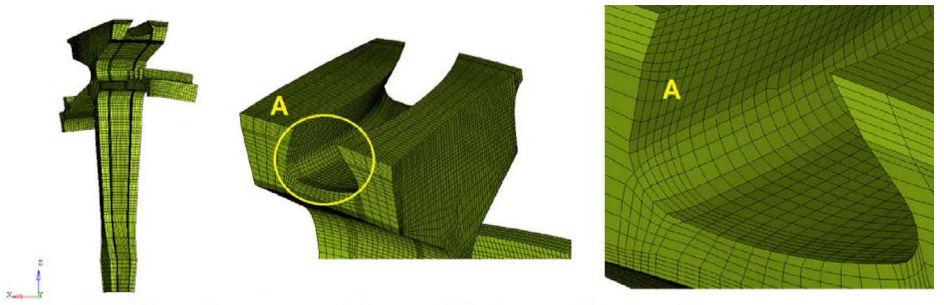

Fig. 23. FE mesh pattern of the modified rotor disc (cyclic symmetry model Ver.2)

Static analysis was performed for models Ver.1 and Ver.2. Equivalent stress states in the rotor blade and the compressor disk are shown in Fig. 24 and 25, respectively. Equivalent stress states in the slot region of the disk are presented in Fig. 26. Displacement states of the entire assembly are compared in Fig. 27. The original design (Ver.0) and its modifications (Ver.1 and Ver.2) are presented in the same scale.

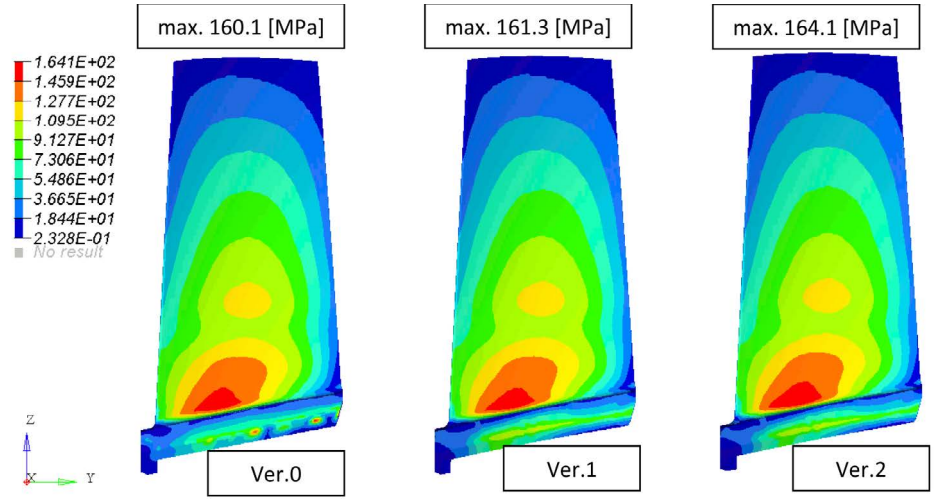

Fig. 24. Equivalent stress states (H-M-H) in the rotor blade. Comparison of model Ver.0 and its modifications Ver.1 and Ver.2

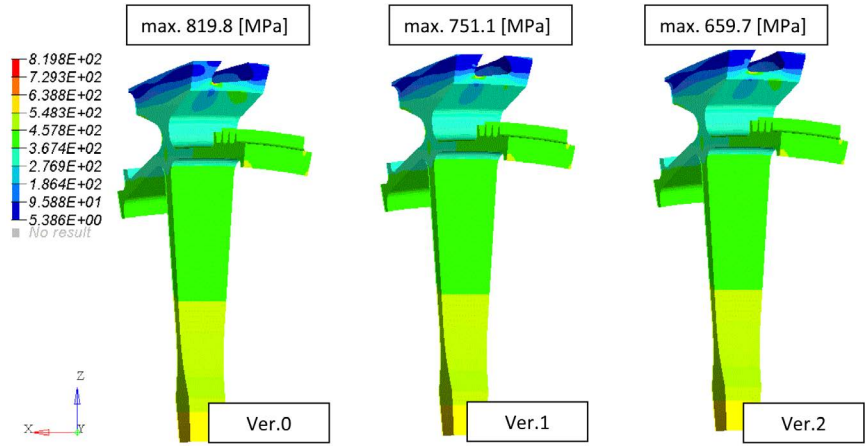

Fig. 25. Equivalent stress states (H-M-H) in the rotor disc. Comparison of cyclic symmetry model Ver.0 and its modifications Ver.1 and Ver.2

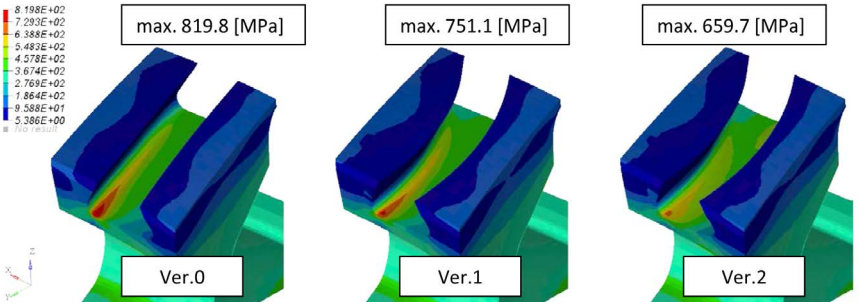

Fig. 26. Equivalent stress states (H-M-H) in the slot region of the rotor disc rim. Maximum stress magnitude is obtained at the bottom of the slot. Comparison of cyclic symmetry model Ver.0 and its modifications Ver.1 and Ver.2

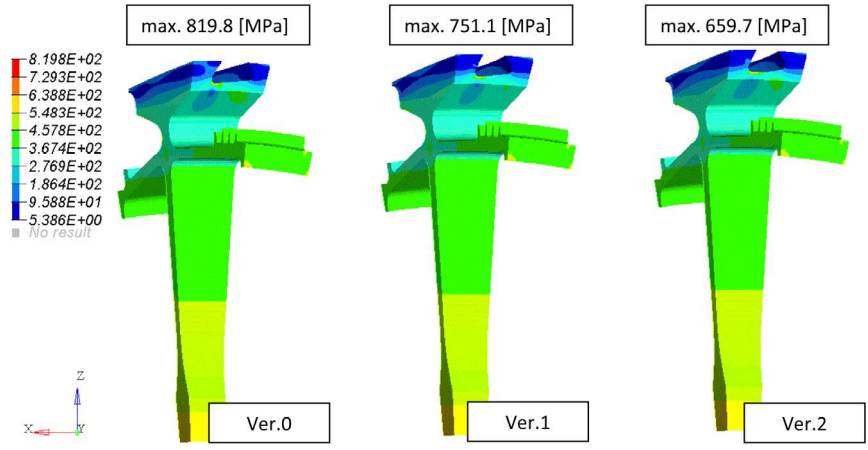

Fig. 27. Radial displacement states in the rotor assembly. Comparison of cyclic symmetry model Ver.0 and its modifications Ver.1 and Ver.2

The maximum stress value obtained in the disc for the modified model Ver.2 is almost 20% lower compared to model Ver.0 (with the original lock geometry). It shows a possibility to increase the safety factor and the fatigue life due to shape modification from a straight to curved root. As a result of the modification, a slight increase (about 4 MPa) in the stress in the rotor blade was noticed but the stress magnitude was definitely lower compared to the yield stress of WT3-1 alloy.

Modal analysis was performed for all models of the rotor assembly. Comparison of the first three modes for the original design (Ver.0) and both lock shape modifications (Ver.1 and Ver.2) are presented in Figs. 28-30.

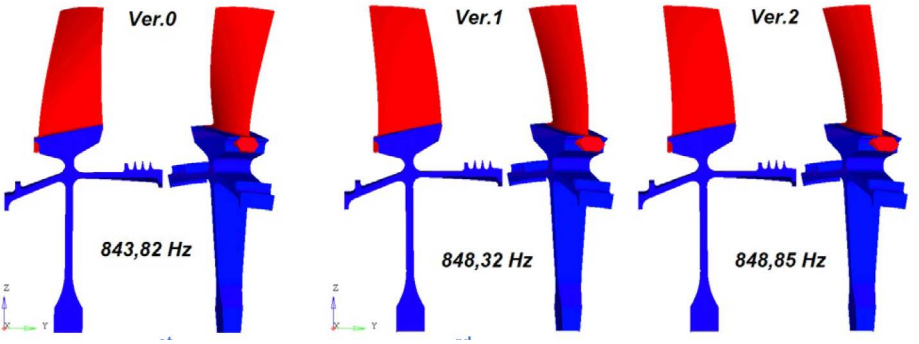

Fig. 28. 1st vibration mode of the 3rd rotor stage. Comparison of cyclic symmetry models Ver.0, Ver.1 and Ver.2

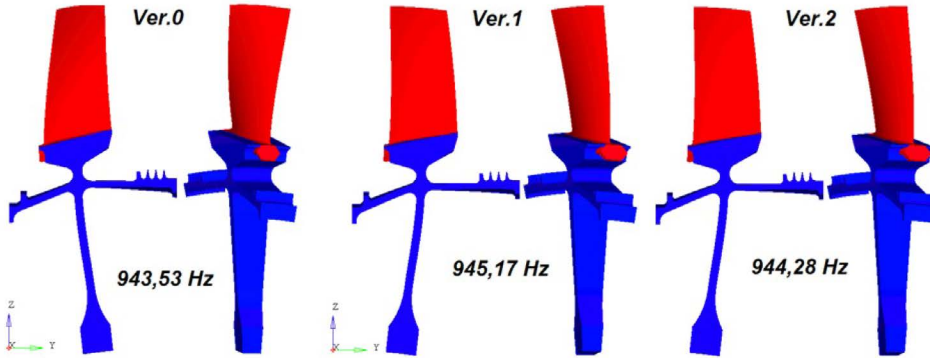

Fig. 29. 2st vibration mode of the 3rd rotor stage. Comparison of cyclic symmetry models Ver.0, Ver.1 and Ver.2

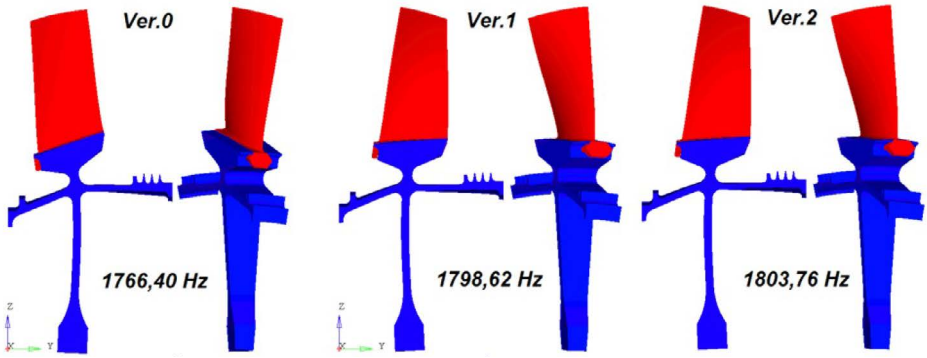

Fig. 30. 3st vibration mode of the 3rd rotor stage. Comparison of cyclic symmetry models Ver.0, Ver.1 and Ver.2

6. SUMMARY AND COMPARISON OF THE RESULTS

The aim of the paper was to design a curved lock (an attachment of the blade to the disk) of the compressor 3rd rotor stage of the K-15 turbine engine. Quasi-static and modal analyses of the rotor assembly were carried out for original (trapezoidal/dovetail) lock geometry and its two modifications. Finite element calculations were performed with LS-Dyna implicit solver using a cyclic symmetry formulation. Due to complex geometries of the analysed models and the relatively long time required to create FE meshes, it was decided to use the HyperMorph module to adjust the original mesh to the modified geometries. Table 4 presents the comparison of all models of the rotor assembly.

Table 4. Comparison of the FE results for original lock geometry (Ver.0) and modifications (Ver.1 and Ver.2)

Maximum equivalent stress (H-M-H) in the rotor blade		
model Ver.0	model Ver.1	model Ver.2
160.1 MPa	161.3 MPa	164.1 MPa
Maximum equivalent stress (H-M-H) in the rotor disk		
model Ver.0	model Ver.1	model Ver.2
819.8 MPa	751.1 MPa	659.7 MPa
Maximum radial displacements of the rotor assembly		
model Ver.0	model Ver.1	model Ver.2
0.358 mm	0.35 mm	0.383 mm

7. CONCLUSIONS

The obtained results (stresses and displacement states) are in line with the theoretical predictions and the results from the literature [1, 11-12, 14-15]. The maximum equivalent H-M-H stress in the blade is about four times lower than the yield stress of the WT3-1 alloy and the maximum stress in the disk is two times lower than the yield stress of Maraging 250 steel.

Stress and displacement states for the modified model Ver.1 are similar to the original design Ver.0. The maximum equivalent stress occurring in the compressor blade for model Ver.1 is slightly higher (about 1%) compared to the original model. On the other hand, the curved geometry of the lock causes a significant reduction in the equivalent stress occurring at the bottom of the compressor disk slot. With regard to the original design, the maximum stress magnitude was reduced by 8.38%.

The last modification (model Ver.2) involved rounding (smoothing) the disk groove/slot. States of stress and displacement obtained for model Ver.2 were similar to the results obtained for model Ver.1. With regard to the original lock geometry, the maximum stress value in the blade was increased by 2.5%, while in the disk it was significantly reduced by 19.53%.

The results of the free vibration study show that the analysed blade root and disk slot modifications do not change the natural frequencies of the assembly, e.g. 3rd frequency was increased by about 2% for model Ver.2 with respect to the original model Ver.0. Therefore, it can be concluded that the proposed modifications of the blade to disc attachment method form a straight to curved shaped lock can be performed without the significant impact on the dynamic parameters of the rotor.

The proposed shape of the curved lock results in a significant reduction of the maximum stress in the disk with respect to the original design, while the stress state in the blade remains almost unchanged. Therefore, further modifications are desirable to reduce stresses in this component. Adjustment of the fillet shape is recognised as the most promising direction of blade optimisation.

The cyclic symmetry formulation allows for a significant computational time reduction. Moreover, morphing of FE mesh in order to adjust it to new geometries significantly decreases time and improves the comfort of developing the modified models.

REFERENCES

[1] Stefan Szczeciński, Włodzimierz Balicki i inni, Lotnicze Zespoły Napędowe, Część 1, Wojskowa Akademia Techniczna, Warszawa, 2009

[2] http://www.tgadvisers.com/news_letter.php?id=5&title=Stress%20Corrosion%20Cracking%20(SCC)%20of%20LP%20Blade%20Rotor%20Attachments

[3] https://nsc.nasa.gov/SFCS/SystemFailureCaseStudy/Details/154

[4] J. Godzimirski, Współczesne i przyszłe materiały konstrukcyjne w lotniczych silnikach turbinowych, Prace Instytutu Lotnictwa, 199, s.95-101, Warszawa 2009,

[5] http://www.titan.su/en/gost-19807-91.html

[6] https://www.aircraftmaterials.com/data/nickel/C250.html

[7] S. Kłysz, Badania stali N18K9M5TPr (maraging) i stopu tytanu WT3-1 w warunkach wysokocyklowego zmęczenia, Kielce 1999

[8] F. Wittel, Mechanics of Building Materials, ETH, Zurich

[9] HyperWorks, Theory Manual, Altair, 2015

[10] Ls-Dyna, Theory Manual, Livermore Software Technology Corporation, May 2007.

[11] J. Jachimowicz, Analiza zespołu sprężarki silnika K-15, Opracowanie wewnętrzne Instytutu Lotnictwa, Warszawa, 1996

[12] W. Wdowiński, Modelowanie i analiza wytrzymałości łopatki III stopnia sprężarki silnika K-15, Praca Dyplomowa, WAT, Warszawa 2016

[13] Loveleen Kumar Bhagi, Pardeep Gupta, Vikas Rastogi, A Brief Review on Failure of Turbine Blades, Proceedings STME-2013 Smart Technologies for Mechanical Engineering, Delhi 25-26 Oct 2013

[14] J. Lipka, Wytrzymałość maszyn wirnikowych, Warszawa, WNT, 1967

[15]. I. Nowotarski, Obliczenia statyczne i dynamiczne turbinowych silnikówlotniczych metodą elementów skończonych, Warszawa, Instytut Lotnictwa, 2001